Research Report

2001-40T

Torque Quality and Comparison of Internal and External Rotor Axial Flux Surface-Magnet Disc Machines

M. Aydin, S. Huang*, T.A. Lipo

Electrical Engineering Department
University of Wisconsin - Madison
1415 Engineering Dr. Room 2559
Madison WI, 53706

*Department of Automation
Shanghai University
149 Yan-Chang Road
Shanghai, 200072, P.R. China

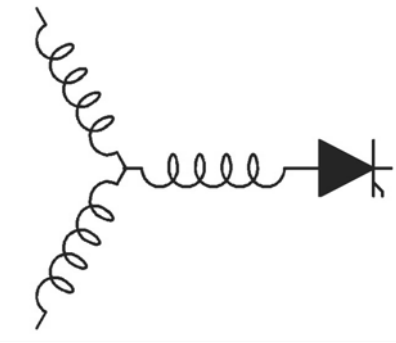

Wisconsin
Electric
Machines &
Power
Electronics
Consortium

University of Wisconsin-Madison
College of Engineering
Wisconsin Power Electronics Research Center
2559D Engineering Hall
1415 Engineering Drive
Madison WI 53706-1691

Torque Quality and Comparison of Internal and External Rotor Axial Flux Surface-Magnet Disc Machines

Metin Aydin, *Member, IEEE*, Surong Huang, and Thomas A. Lipo, *Fellow, IEEE*

***Abstract*—In this paper, pulsating torque components of permanent magnet machines and pulsating torque minimization techniques are discussed for axial flux surface-magnet disc-type PM machines. The pulsating torque analysis describing general instantaneous electromagnetic torque equation and torque ripple factor is briefly provided in order to analyze torque ripple component. Detailed finite-element analyses focusing on the minimization of cogging and torque ripple components using several techniques are also given. A detailed comparison of the two techniques is also illustrated in this paper.**

***Index Terms*—AC motors, permanent magnet machines, permanent magnet motors, traction motors.**

I. Introduction

AXIAL flux permanent magnet (PM) disc-type nonslotted and slotted internal-rotor–external-stator (AFIR type) and internal-stator–external-rotor (TORUS type) machines have recently found a growing interest for high-performance drive applications [1]–[4]. These machines can be designed for higher torque-to-weight ratio and higher efficiency and can be considered as a significant advantage over conventional PM machines. Torque quality of AFPMs is an important matter for low-noise smooth-torque PM disc machines and directly related to pulsating torque component. Pulsating torque consists of two components, namely 1) cogging torque and 2) "torque ripple". Cogging torque arises from the variation of the magnetic permeance of the stator teeth and the slots above the permanent magnets. The presence of cogging torque is a concern in the design of PM machines because it adds unwanted harmonics to the pulsating torque. Torque ripple occurs as a result of fluctuations of the field distribution and the armature magnetomotive force (MMF). At high speeds, torque ripple is usually filtered out by the system inertia. However, at low speeds or gearless-motor direct-drive systems, torque ripple produces noticeable effects that may not be tolerable in smooth-torque and low-noise applications [1]–[4].

Manuscript received August 29, 2003; revised August 16, 2005. Abstract published on the Internet March 18, 2006. This work was supported by the Naval Surface Warfare Center under Grant N00014-98-1-0807.

M. Aydin is with Technical Center TC-G 855, Caterpillar Inc., Peoria, IL 61656-1875 USA (e-mail: maydin@ieee.org).

S. Huang is with the Department of Automation, Shanghai University, Shanghai 200072, China (e-mail: srhuang@sh163.net).

T. A. Lipo is with the Department of Electrical and Computer Engineering, University of Wisconsin, Madison, WI 53706 USA (e-mail: lipo@engr.wisc.edu).

Digital Object Identifier 10.1109/TIE.2006.874268

The torque quality assessment of different machine types is a challenging task because the assessment consider not only torque density (both torque-to-volume and torque-to-weight ratios) but also the pulsating torque. A mathematical approach to torque quality should include a harmonic analysis of the entire electric drive system. The main harmonic sources of the pulsating torque are the effects of slotting the stator, which results in the production of permeance harmonics and placement of the windings and magnets as well as the stator slot and pole number combinations.

This paper relates to the torque quality of axial flux PM (AFPM) machines. Section II discusses the pulsating torque minimization techniques for PM machines. The nonslotted and slotted axial flux disc-type PM machine structures are introduced in Section III. Sections IV and V present pulsating torque investigations of PM machines by using mathematical and finite-element (FE) approaches. Special attention is paid to torque ripple minimization in the disc machines. Finally, a detailed comparison of the two approaches and the conclusions are illustrated in Sections VI and VII.

II. PM Motor Design Techniques for Pulsating Torque Minimization

The definitions of the torque components used in this paper are given in the following list.

1) Cogging torque is the pulsating torque component produced by the variation of the air gap permeance or reluctance of the stator teeth and slots above the magnets as the rotor rotates. No stator excitation is involved in cogging torque production.
2) Torque ripple is the pulsating torque component generated by the stator MMF and rotor MMF. In surface-mounted PM machines, torque ripple is mainly created by the interaction between the MMF caused by the stator windings and the MMF caused by the rotor magnets because there exists no rotor reluctance variation.
3) Pulsating torque is the sum of both cogging and torque ripple components.
4) Total torque is the sum of average torque and pulsating torque components.

Sinusoidal PM motors have many similarities with other types of ac motors. For example, if the back electromotive force (EMF) of the PM machine and current waveform are perfectly

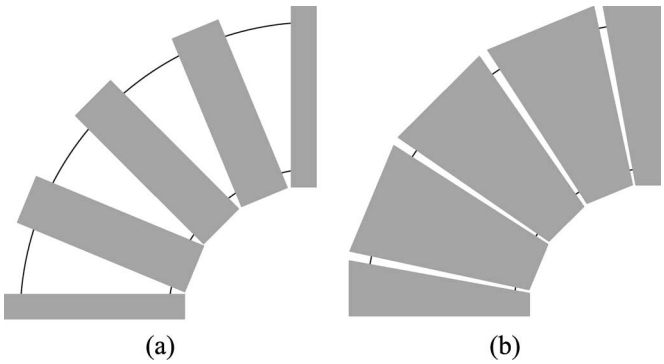

Fig. 1. (a) Rectangular and (b) pie-shaped windings used in slotless AFPM machines.

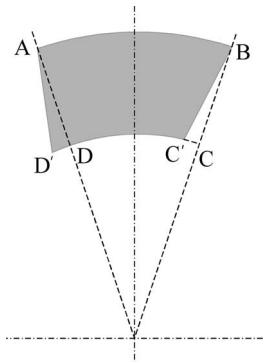

Fig. 2. Skewed and nonskewed magnet. Magnet A B C D is skewed to A B C′ D′.

sinusoidal, it results in smooth torque production. The requirement for the sinusoidal PM machines is that the air gap flux density should vary sinusoidally along the air gap when the stator of the machine is not excited (no-load case). The second requirement is that the stator windings of the PM machine should be distributed sinusoidally around the air gap. Any nonideal situation such as a disturbed stator current waveform arising from the converter or disturbed back-EMF waveform arising from the nonuniform air gap will cause nonsinusoidal current and air gap flux density waveforms that result in undesired pulsating torque components in the machine. In other words, the machine torque is proportional to the square of the flux density in the air gap. If the air gap flux density waveform is disturbed, pulsating torque becomes unavoidable.

There exist many techniques in the literature for the minimization of pulsating torque components of disc-type PM machines [5]–[9]. In general, these minimization techniques can be classified into two major categories. 1) The first one comprises the techniques for modifying machine design so that the pulsating torque component is minimized and smooth torque goal is achieved. 2) The second category is based upon control schemes for modifying the stator excitation waveform to obtain smooth torque. In this paper, the focus will be placed on machine-design-based techniques to achieve smooth torque operation.

The most effective means to minimize torque pulsations relies on proper machine design. Many techniques (such as using appropriate stator winding type, introducing rectangular or pie-shaped back-to-back-connected gramme-type stator windings in slotless topologies, and skewing either stator slots or rotor magnets, rotor shifts, and magnet shifts) are used to achieve this goal from a machine design perspective.

First, gramme-type back-to-back-connected windings are used in slotless axial flux machines (AFMs), and they help reduce the torque ripple component. Replacing the rectangular winding with a sector-shaped winding helps even more in reducing the torque ripple component of the slotless topologies, providing better stator utilization. Both winding types are illustrated in Fig. 1(a) and (b).

Second, skewing either the stator slots or rotor magnets is one of the effective techniques used in PM machines to reduce the pulsating torque components. A skewed and unskewed magnet piece for an AFM is illustrated in Fig. 2. However, this technique has some drawbacks such as giving rise to average loss reduction and an increasing leakage inductance during flux weakening operation.

Third, a short-pitched winding can be used to reduce the torque ripple of the machine by reducing high-order harmonics. For instance, a TORUS machine designed with short-pitched windings provides better results in terms of torque quality than a TORUS machine designed with back-to-back connected windings. Fractional slot windings can also be used for low-speed applications with low number of slots per pole per phase. Moreover, the cogging torque of a PM machine can be minimized by properly designing pole arc ratio, given that the cogging torque could be a significant source of pulsating torque. One of the common techniques used to reduce the cogging torque in AFMs besides skewing and pole arc is introducing magnet shifts. With this simple technique, cogging torque reduction is accomplished by changing the magnet symmetry. In addition to these techniques, there exist other methods to minimize the cogging torque components, such as paralleling the magnet sides, alternating pole arcs in facing rotors, reducing the slot openings, and placing magnetic slot wedges. Each technique has certain benefits and drawbacks. However, skewing is the only technique that is used in the rotor to improve the torque quality of AFMs in this paper.

III. AFPM Disc-Type Motor Structures

AFPM disc machines can be constructed in different forms. The structures investigated in this paper have either a single stator sandwiched between two disc rotors (the TORUS topology) or a single rotor sandwiched between two stators (the AFIR topology). The axial flux topologies investigated in this paper are shown in Fig. 3(a)–(d), and the abbreviations are illustrated in Table I.

The external-rotor–internal-stator nonslotted and slotted TORUS machines shown in Fig. 3(a) and (b) have a single stator and two PM rotor discs. The stators are realized by a tape wound core with ac polyphase windings. Air gap windings, which are wrapped around the stator core with a back-to-back connection, and evenly distributed back-to-back connected windings are used for slotless and slotted TORUS topologies, respectively. The rotor structure is formed by a fan-shaped

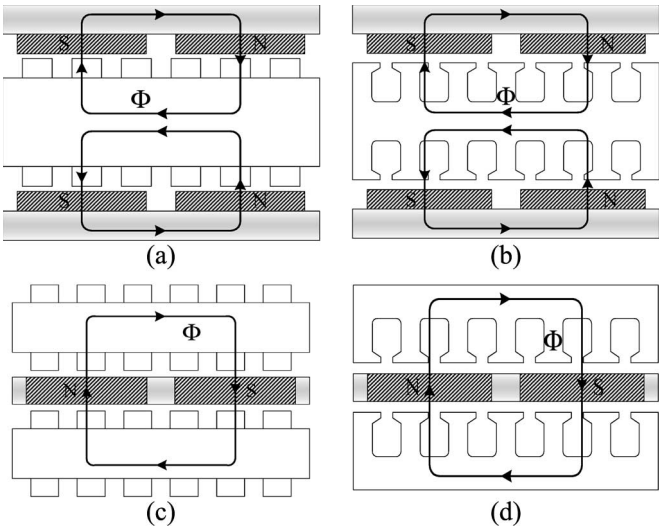

Fig. 3. AFPM disc-type motor structures: (a) slotless TORUS, (b) slotted TORUS, (c) slotless AFIR, and (d) slotted AFIR machines.

TABLE I
RADIAL AND AXIAL FLUX PM MACHINE STRUCTURES

Abbreviation	Radial and Axial Flux Surface Magnet PM Machine Types
RFSM-NS	Radial flux surface mounted PM non-slotted motor
RFSM-S	Radial flux surface mounted PM slotted motor
TORUS-NS	Axial flux external rotor internal stator PM non-slotted motor
TORUS-S	Axial flux external rotor internal stator PM slotted motor
AFIR-NS	Axial flux internal rotor external stator PM non-slotted motor
AFIR-S	Axial flux internal rotor external stator PM slotted motor

surface-mounted axially magnetized NdFeB permanent magnets, rotor core, and shaft.

The AFIR-type machines have two stator discs and a single rotor disc, as shown in Fig. 3(c) and (d). The stator structures are realized by either a slotless or slotted tape wound core with ac polyphase windings. Gramme-type windings are wrapped around the stator core for the slotless machine and short-pitched lap ac windings for the slotted topology. The winding pitch is designed to be 5/6 so that the air-gap harmonics can be minimized. The rotor structures of the AFIR machines are formed by the axially magnetized surface magnets and a shaft. It should be mentioned that the portions between the windings in nonslotted topologies are filled with epoxy resin so as to form a solid rotor structure, increase the robustness of the structure, and provide better heat transfer. The parameters of both TORUS- and AFIR-type machines analyzed in this paper are given in Table II.

The basic flux paths of the TORUS and AFIR topologies are shown in Fig. 4(a) and (b), respectively. As can be shown in Fig. 4(a) (for the TORUS machines), the N magnets drive flux into the stator core through the air gaps. The flux then travels circumferentially along the stator core, returns across the air gaps, and then enters the rotor core through the opposite polarity of the magnets. In the AFIR-type machines shown in Fig. 4(b), the magnets with the polarity of N drive flux across the upper air gap into the upper stator core. The flux then travels circumferentially along the upper stator core, returns to the upper air gap, then enters the lower stator core through the S pole of the magnets, and closes its path.

TABLE II
PARAMETERS OF THE AFPM MACHINES

	TORUS-NS	TORUS-S	AFIR-NS	AFIR-S
Rated speed [rpm]	1200	1200	1200	1200
Number of poles	6	6	6	6
Number of slots	--	36	--	36
Current density [A/mm^2]	9	9	6.6	6.2
Outer radius [mm]	686.5	519.6	786.9	530.9
Inner radius [mm]	311.3	259.8	362	276.1
Stator core [mm]	53.8	89.1	34.1	51.2
Rotor core [mm]	21.7	50.6	0	0
Magnet thickness	9.1	12.0	21.2	19.0
Airgap [mm]	1	1	1	1

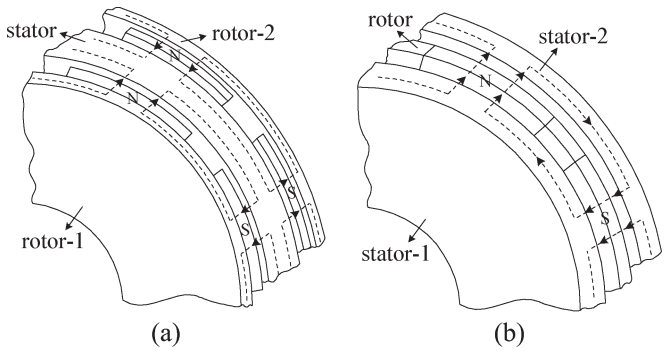

Fig. 4. Three-dimensional (3-D) flux paths of the (a) TORUS- and (b) AFIR-type topologies.

IV. PULSATING TORQUE ASSESSMENT OF AFMS USING A MATHEMATICAL APPROACH

In general, if stator leakage inductance and resistance are neglected, the general instantaneous electromagnetic torque for any electrical machine can be expressed as

$$T_{\rm em}(t) = \frac{1}{\omega_m}\sum_{j=1}^{m} e_j(t) i_j(t) \tag{1}$$

where j is the order of machine phase, m is the number of machine phases, $e_j(t)$ and $i_j(t)$ are the phase back EMF and the phase current in phase j, respectively, and ω_m is the rotor angular speed.

In the electromagnetic and torque ripple analyses, it was assumed that the motor is unsaturated, armature reaction is neglected, and the fundamental components of the phase currents and the corresponding phase back EMFs are maintained in phase. For the Y-connected three-phase stator winding, the back EMF in phase a can be written as

$$e_a = E_1 \sin\omega t + E_3 \sin 3\omega t + E_5 \sin 5\omega t + E_7 \sin 7\omega t + \cdots \tag{2}$$

and the current in phase a can be written as

$$i_a = I_1 \sin\omega t + I_5 \sin 5\omega t + I_7 \sin 7\omega t + I_{11} \sin 11\omega t + \cdots \tag{3}$$

where E_n is the nth time harmonic peak value of the phase back EMF, which is produced by the nth space harmonic of the air gap magnetic flux density $B_{\rm gn}$, and I_n is the nth time harmonic peak value of the armature phase current, which depends on the armature phase current waveform. Moreover, it should be noted that there is no neutral connection used in the winding so that

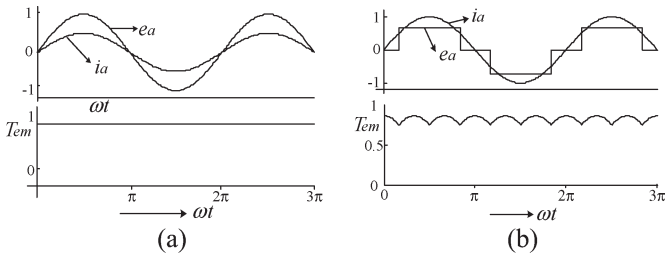

Fig. 5. Torque ripple for (a) sinusoidal and (b) square-wave current cases.

harmonics of multiples of three do not exist. The product $e_a i_a$ is composed of an average component and even-order harmonics for phase a. The total instantaneous torque contributed by each machine phase is proportional to the product of phase back EMF and phase current. The sum $(e_a i_a + e_b i_c + e_c i_c)$ will contain an average component and harmonics of the order of six, and the other harmonics are eliminated. The final instantaneous electromagnetic torque equation becomes

$$\begin{aligned} T_{\rm em}(t) &= T_0 + T_6 \cos 6\omega t + T_{12} \cos 12\omega t \\ &\quad + T_{18} \cos 18\omega t + \cdots \\ &= T_0 + \sum_{n=1}^{\infty} T_{6n} \cos n6\omega t \end{aligned} \tag{4}$$

where T_0 is the average torque, T_{6n} is harmonic torque components, and $n = 1, 2, 3, \ldots$ The fundamental and first three harmonic torque components are given from (5)–(8)

$$\begin{aligned} T_0 &= \frac{3}{2\omega_m}[E_1 I_1 + E_5 I_5 + E_7 I_7 \\ &\quad + E_{11} I_{11} + E_{13} I_{13} + \cdots] \end{aligned} \tag{5}$$

$$\begin{aligned} T_6 &= \frac{3}{2\omega_m}[I_1(E_7 - E_5) + I_5(E_{11} - E_1) \\ &\quad + I_7(E_1 + E_{13}) + I_{11}(E_5 + E_7) + \cdots] \end{aligned} \tag{6}$$

$$\begin{aligned} T_{12} &= \frac{3}{2\omega_m}[I_1(E_{13} - E_{11}) + I_5(E_{17} - E_7) \\ &\quad + I_7(E_{19} - E_5) + I_{11}(E_{23} - E_1) + \cdots] \end{aligned} \tag{7}$$

$$\begin{aligned} T_{18} &= \frac{3}{2\omega_m}[I_1(E_{19} - E_{17}) + I_5(E_{23} - E_{13}) \\ &\quad + I_7(E_{25} - E_{11}) + I_{11}(E_{29} - E_7) + \cdots]. \end{aligned} \tag{8}$$

In the ideal case, if the back EMFs and the armature phase currents are sinusoidal, the electromagnetic torque is constant and no torque ripple exists, which is illustrated in Fig. 5(a). If one of these quantities is a square wave, then the resultant torque will include torque pulsations, as shown in Fig. 5(b).

Because almost all practical stator windings and PM field distributions have some significant winding harmonics and flux density harmonics, induced phase back EMFs are not sinusoidal and contain high-order harmonics. As a result, torque ripple exists even with a sinusoidal phase current source.

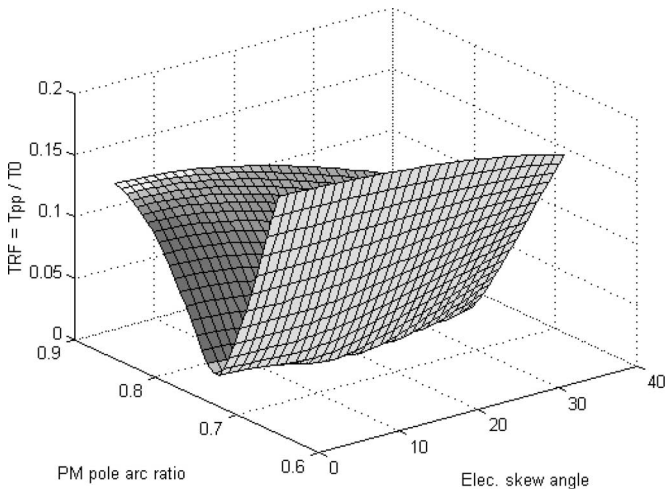

Fig. 6. TRF of the slotless TORUS machine with rectangular winding as a function of pole arc and magnet skew angle.

The torque ripple factor (TRF) can be defined as the ratio of peak-to-peak torque ripple to average torque and expressed as

$$\text{TRF} = \frac{T_{\rm pp}}{T_0} = \frac{2\sqrt{T_6^2 + T_{12}^2 + T_{18}^2 + \cdots}}{T_0} \tag{9}$$

where $T_{\rm pp}$ is the peak-to-peak torque ripple. For the sinusoidal phase current case, the TRF expression takes the form of (10), shown on the bottom of the page, where

$$\frac{K_{\rm hn}}{K_{h1}} = \frac{K_{\rm wn} \cdot K_{\rm sn} \cdot K_{\rm fn} \cdot K_{\rm osn}}{K_{w_1} \cdot K_{s_1} \cdot K_{f_1} \cdot K_{os1}} = \frac{E_n}{E_1} \tag{11}$$

and $K_{\rm hn} = K_{\rm wn} K_{\rm sn} K_{\rm fn} K_{\rm osn}$ is the nth harmonic factor, $K_{\rm wn}$ is the nth harmonic winding factor, $K_{\rm fn}$ is the nth PM field harmonic form factor, $K_{\rm sn}$ is the nth harmonic rotor PM skew factor, and $K_{\rm osn}$ is the nth harmonic open slot factor.

The analysis procedure summarized here can be applied to any of the surface-mounted PM machine. The slotless TORUS machine is given as the sample machine in the following pulsating torque analysis. First, a gramme-type rectangular ac winding is used in the design, and the TRF is investigated for different magnet skew angles and pole arc ratios. The winding structure is then replaced with a pie-shaped winding to smooth the torque ripple of the slotless TORUS machine. Optimum design point can be obtained for minimum TRF after this procedure.

Fig. 6 shows the TRF plot as a function of magnet pole arc ratio and magnet skew angle for rectangular back-to-back connected stator winding case. It is clear from the figure that the TRF has a minimum near a PM pole arc ratio of 0.8 and a skew angle of 31 electrical degrees.

$$\text{TRF} = 2\frac{\sqrt{(K_{h_7} - K_{h_5})^2 + (K_{h13} - K_{h11})^2 + (K_{h19} - K_{h17})^2 + \ldots}}{K_{h1}} \tag{10}$$

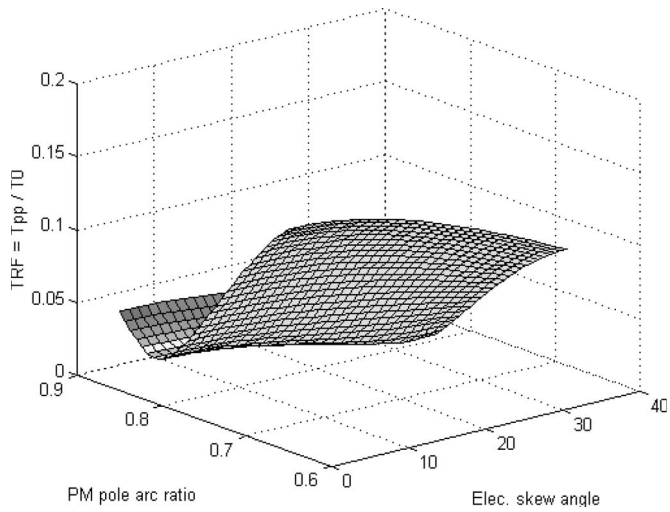

Fig. 7. TRF of the slotless TORUS machine with pie-shaped winding as a function of pole arc and magnet skew angle.

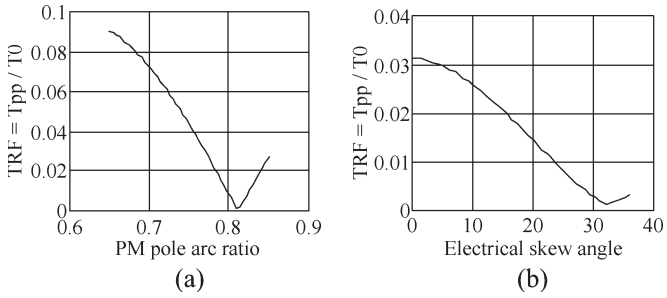

Fig. 8. TRF of the slotless TORUS machine with pie-shaped winding as a function of (a) pole arc and (b) magnet skew angle.

When the stator ac winding structure is replaced with a pie-shaped gramme winding, which provides better stator utilization compared to the rectangular winding, the torque ripple of the machine becomes smaller, as shown in Fig. 7. The TRF has a minimum at a PM pole arc ratio of 0.81 and a skew angle of 31 electrical degrees. The optimum skew angle and magnet pole arc ratio is also shown clearly in Fig. 8(a) and (b) for this case.

The same analysis has been completed for all the radial and AFPM machines described earlier in this paper. A summary of the results with the rectangular and pie-shaped windings for different skew angles and PM pole arc ratios is provided in Tables III and IV for the TORUS and AFIR topologies, respectively. The TRFs for different magnet pole arc ratios and skew angles as well as the unskewed case around the minimum TRF are illustrated in the tables. It can be observed from the tables that torque ripple is very sensitive to PM pole arc ratio $(\alpha_{\rm i})$ and skew angle $(\theta_{\rm skew})$, and precision of these parameters is very important for smooth-torque PM motors.

V. Pulsating Torque Assessment of Radial and Axial Flux Machines Using 3-D Finite-Element Analysis (FEA)

FEA can accurately analyze the models involving permanent magnets of any shape and material. There is no need to calculate the reluctances and inductances using circuit-type analytical methods because these values can simply be extracted from the FEA. One important advantage of using FEA is the ability to calculate torque variations, such as cogging torque, torque ripple, and total torque with changes in rotor position. The main purpose of this analysis is to find out and minimize the torque ripple of the radial and axial flux machines using some of the techniques mentioned earlier and compare the results with the mathematical approach discussed in the previous section.

TABLE III
TRF for TORUS-NS and TORUS-S Machines

	$\alpha_{\rm i}$	**0.79**	**0.80**	**0.81**	**0.82**
TORUS-NS rectangular type	$\theta_{skew}=0$	0.102	0.113	0.121	0.129
	$\theta_{skew}=30$	0.046	0.057	0.067	0.077
	$\theta_{skew}=31$	0.043	0.054	0.064	0.074
	$\theta_{skew}=32$	0.040	0.051	0.062	0.071
TORUS-NS pie shaped	$\theta_{skew}=0$	0.043	0.037	0.032	0.029
	$\theta_{skew}=30$	0.021	0.014	0.007	0.001
	$\theta_{skew}=31$	0.020	0.013	0.006	0.001
	$\theta_{skew}=32$	0.019	0.012	0.006	0.002
TORUS-S	$\theta_{skew}=0$	0.337	0.346	0.330	0.360
	$\theta_{skew}=30$	0.048	0.041	0.036	0.033
	$\theta_{skew}=31$	0.042	0.034	0.028	0.024
	$\theta_{skew}=32$	0.039	0.030	0.022	0.018

TABLE IV
TRF for AFIR-NS and AFIR-S Machines

	$\alpha_{\rm i}$	**0.79**	**0.80**	**0.81**	**0.82**
AFIR-NS rectangular type	$\theta_{skew}=0$	0.100	0.111	0.120	0.127
	$\theta_{skew}=30$	0.045	0.056	0.066	0.076
	$\theta_{skew}=31$	0.042	0.053	0.064	0.073
	$\theta_{skew}=32$	0.040	0.051	0.061	0.070
AFIR-NS pie shaped	$\theta_{skew}=0$	0.043	0.037	0.032	0.029
	$\theta_{skew}=30$	0.021	0.014	0.007	0.001
	$\theta_{skew}=31$	0.020	0.013	0.006	0.001
	$\theta_{skew}=32$	0.019	0.012	0.006	0.002
AFIR-S	$\theta_{skew}=0$	0.317	0.331	0.317	0.349
	$\theta_{skew}=30$	0.027	0.030	0.032	0.033
	$\theta_{skew}=31$	0.019	0.022	0.023	0.024
	$\theta_{skew}=32$	0.015	0.017	0.017	0.019

A. Radial Flux Surface Mounted (RFSM)-Type Topologies

The FE calculations of the 200-hp six-pole machine are carried out using Maxwell two-dimensional (2-D) and 3-D software with skewed and unskewed rotor magnet cases for different rotor positions. The peak-to-peak torque ripple for slotless RFSM machine was found to be 0.063 p.u. with unskewed PMs and 0.035 p.u. with skewed PMs. The same analysis was carried out for a conventional radial flux slotted PM machine, which is used as the reference machine in the comparison. The cogging and torque ripple analyses were performed for different cases such as modified slot, with magnetic slot wedge in the slot openings, and with skewed and unskewed rotor magnets. Pulsating torque was also tried to be minimized. In the final design, the peak-to-peak torque ripple was found to be 0.059 p.u.

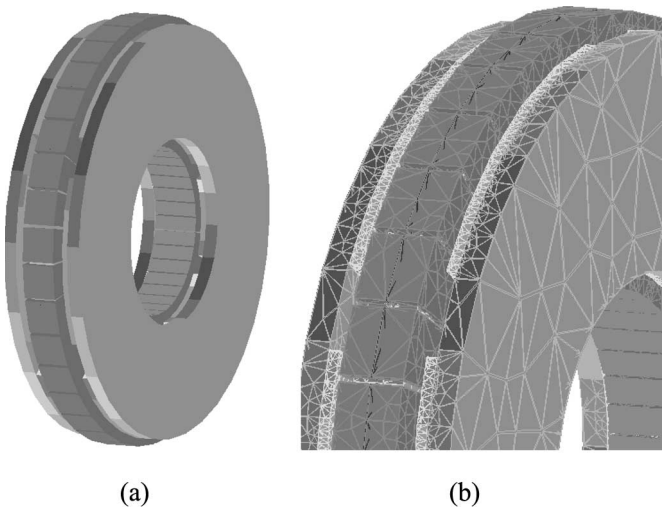

Fig. 9. One of the FEA models created for (a) slotless TORUS machine and (b) the typical 3-D FEA mesh for the same model.

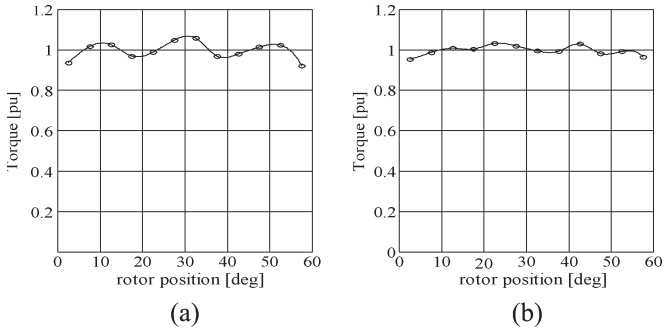

Fig. 10. Total torque of the TORUS-NS machine (a) with rectangular back-to-back-connected winding and without skewed magnets and (b) with pie-shaped back-to-back-connected winding and skewed rotor magnets.

B. TORUS-Type Topologies

Because no slots exist in the slotless TORUS topology, the cogging torque is negligible, and the pulsating torque component of the machine is equal to the torque ripple component. FEA models were created, and calculations were carried out for different rotor positions over one pole for the same 200-hp six-pole machine with skewed and unskewed rotor magnets. One of the models created with unskewed magnets and pie-shaped gramme-type coils as well as the 3-D FE mesh was illustrated in Fig. 9. The FE simulation takes about 31 min, and 168.521 3-D elements are generated to give accurate torque output.

First, the total torque of the machine at rated power with rectangular back-to-back connected stator winding and with unskewed rotor PMs was plotted over one pole and is shown in Fig. 10(a). The peak-to-peak torque ripple was found to be 0.12 p.u. Second, the winding structure was changed to a pie-shaped gramme-type structure to reduce the torque ripple by obtaining better stator utilization, and the torque ripple was reduced to 0.046 p.u. of the average (rated) torque.

Third, the rotor magnets are skewed by the optimum magnet skew angle with the pie-shaped back-to-back connected winding structure. It was found that the torque ripple was reduced to 0.033 p.u. The resultant torque ripple plot is shown in Fig. 10(b). The total torque ripple reduction from step 1 to step 3 becomes 72.5% for this machine.

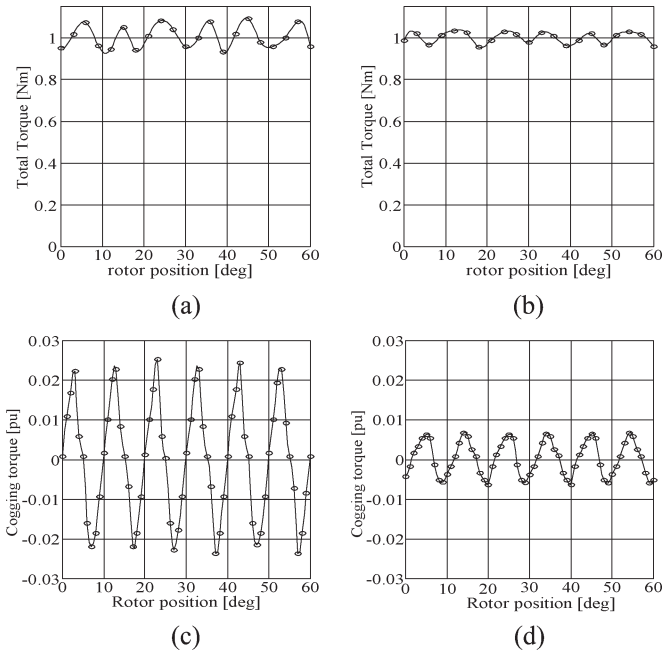

Fig. 11. Cogging torque of the TORUS-S machine (a) without and (b) with skewed rotor magnets and output torque of the TORUS-S machine (c) with rectangular gramme-type winding and without skewed magnets, and (d) with pie-shaped gramme-type winding and without skewed rotor magnets.

In the TORUS-S machine, pulsating torque comprises both cogging and torque ripple components unlike that in the slotless TORUS topology. Fig. 11(a) and (b) shows the cogging torque plots with unskewed/skewed rotor magnet cases. FEA calculations reveal that the peak-to-peak cogging torque for the TORUS-S topology without skewing the magnets is 0.043 p.u. When the rotor magnets were skewed by the optimum skew angle, the cogging torque became 0.0125 p.u. Hence, skewing the rotor PMs reduced the cogging torque of the slotted TORUS machine by nearly 79.0%.

The total torque behavior of the slotted TORUS machine is displayed in Fig. 11(c) and (d). The torque ripple of the machine was found to be 0.156 p.u. peak-to-peak for the unskewed rotor magnet case and 0.075 p.u. peak-to-peak for the skewed magnet case. This results in a torque ripple reduction of 51.3% by simply skewing the magnets.

C. AFIR-Type Topologies

3-D FEA is again used for the AFIR machines to investigate the torque quality for the same power ratings. The same torque ripple analysis was carried out for the slotless AFIR topology for both rectangular and pie-shaped gramme-type windings with unskewed magnets. The torque ripple with rectangular gramme-type winding with unskewed magnets was 0.105 p.u., whereas it was calculated to be 0.055 p.u. with the pie-shaped winding and with unskewed magnets, as shown in Fig. 12(a) and (b). Thus, the torque ripple reduction from case 1 to case 2 was found to be 52%.

The torque quality of the slotted AFIR machine was also examined by analyzing cogging and torque ripple components

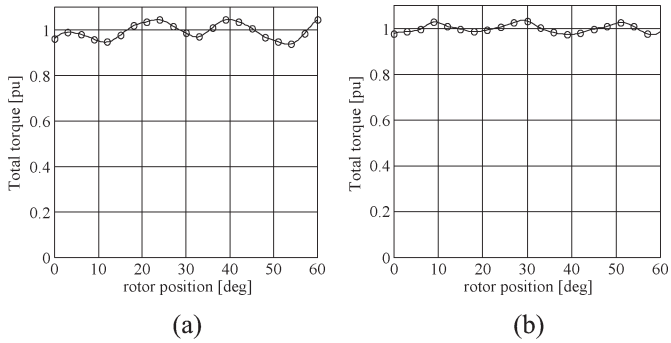

Fig. 12. Total torque of the nonslotted internal-rotor-type machine (a) with rectangular gramme-type winding and without skewed rotor magnets, and (b) with pie-shaped winding and without skewed rotor magnets.

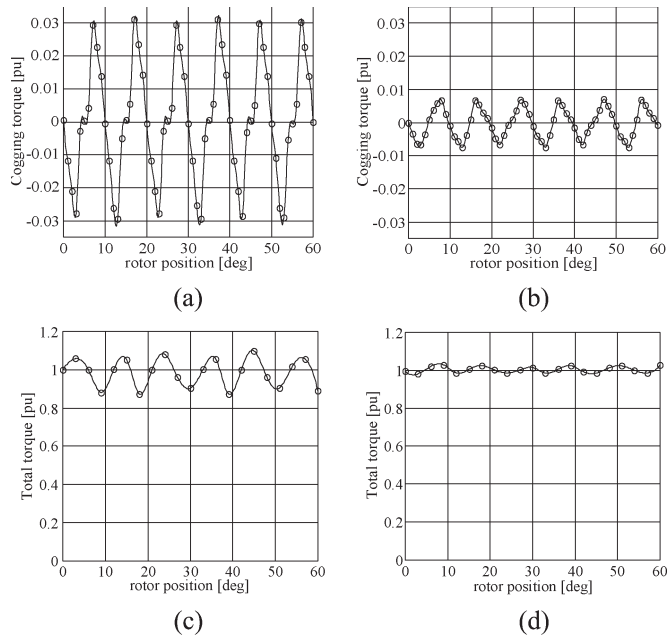

Fig. 13. Cogging torque of the nonslotted internal-rotor-type machine (a) without and (b) with skewed rotor magnets and total torque of the AFIR-S machine at a rated load (c) without and (d) with skewed rotor magnets.

in Fig. 13(a) and (b). The peak-to-peak cogging torques of the AFIR-S topology were found to be 0.062 p.u. and 0.013 p.u. with unskewed and skewed magnets. Again, the optimum skew angle found in the TRF analysis was used in the FEA models. The effect of skewing on torque ripple is clearly shown in Fig. 13(c) and (d). It can be observed that the torque ripple has a peak-to-peak value of 0.383 p.u. for the unskewed magnet case and 0.081 p.u. for the skewed magnet case. This leads to a torque ripple reduction of 78.8% for this machine.

VI. Comparison of Torque Quality Using Both Mathematical and FE Approaches

The summary of the torque analysis completed in this paper is shown in Tables V and VI. Fig. 14(a) and (b) shows the peak-to-peak values of cogging and torque ripple comparison obtained from the FEA for both nonslotted and slotted topologies, respectively. It can be observed from the tables and figures that the cogging torque is the highest for the conventional PM machine (RFSM-S). In general, nonslotted machines have less

TABLE V
Cogging Torque Comparison of Radial and Axial Flux Machines Using FE Approach

	Without skewed rotor PMs [pu]	With skewed rotor PMs [pu]
RFSM-NS	0	0
RFSM-S	0.26 / 0.067*	0.088
TORUS-NS	0	0
TORUS-S	0.043	0.0125
AFIR-NS	0	0
AFIR-S	0.062	0.013

TABLE VI
Torque Ripple Comparison of Radial and Axial Flux Machines Using FE Approach

	with rectangular shaped winding	with pie shaped winding	with skewed PMs
RFSM-NS	0.063	---	0.035
RFSM-S	0.429 / 0.101*	---	0.059
TORUS-NS	0.120	0.046	0.033
TORUS-S	0.156	---	0.075
AFIR-NS	0.105	0.055	---
AFIR-S	0.383	---	0.081

*Slot wedge is used

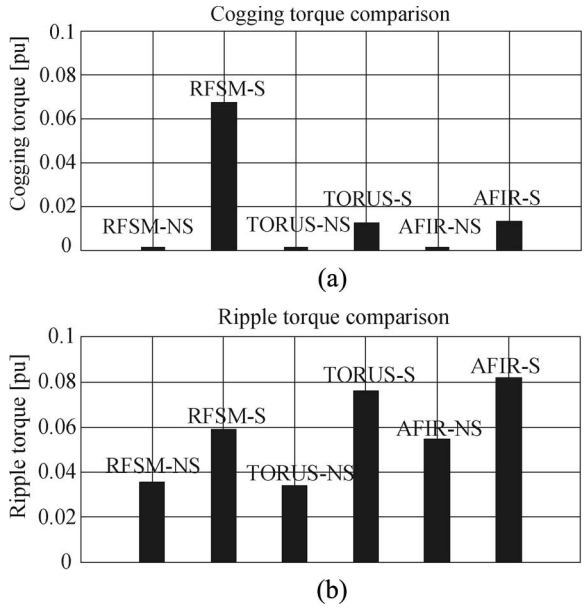

Fig. 14. Cogging torque (a) and torque ripple (b) comparison for radial and axial flux surface-magnet PM machines.

torque ripple than slotted topologies. As for the nonslotted AFMs, the slotless TORUS machine has the lowest torque ripple compared to the other topologies, and the slotless RFSM machine has the highest torque ripple component compared to other nonslotted machines.

Table VII shows a summary of the results obtained from the mathematical TRF analysis. The table shows the torque ripple per unit for different machines with skewed and unskewed PMs. As shown in the comparison between the two approaches, results obtained from the mathematical approach agree well with the FE approach for slotless topologies because the armature reaction of nonslotted topology machines is quite small. However, the armature reaction of slotted topologies strongly interferes with the air-gap flux field, which results in stronger

TABLE VII
TORQUE RIPPLE COMPARISON OF RADIAL AND AXIAL FLUX MACHINES USING MATHEMATICAL APPROACH

	Non-slotted with rectangular shaped winding or slotted with double layer lap winding			Non-slotted with pie shaped winding or slotted with back to back connected winding		
	without skewed PM	with skewed PM	TRS factor*	without skewed PM	with skewed PM	TRS factor*
RFSM-NS	0.037	0.014	2.64	---	---	---
RFSM-S	0.37	0.031	11.9	---	---	---
TORUS-NS	0.11	0.057	1.93	0.037	0.014	2.64
TORUS-S	0.33	0.030	11.0	0.35	0.041	8.53
AFIR-NS	0.11	0.056	1.96	0.037	0.014	2.64
AFIR-S	0.33	0.029	11.3	---	---	---

*Torque ripple sensitivity (TRS)=Ripple torque at non-skewed PM/Ripple torque at skewed PM

harmonic components. Therefore, torque ripple by mathematical approach is slightly less than that by the FEA approach. Besides, it was assumed that the motor is unsaturated and armature reaction is neglected in the mathematical analysis. Because the effect of armature reaction is significant in slotted machines, a small discrepancy between the TRF and FEA approaches can be expected for slotted AFMs. Torque ripple sensitivity (TRS) to skew angle is also illustrated in the table. The table shows that peak-to-peak torque ripple in slotless topologies is less sensitive to skew angle change than that in slotted topologies because of the armature reaction effect.

VII. CONCLUSION

This paper has described the comparison of internal- and external-rotor AFPM machines in terms of torque quality using two different approaches. A study of pulsating torque analysis using mathematical approach was also briefly clarified. A detailed 2-D and 3-D FEA for AFMs to predict both cogging and torque ripple behaviors was illustrated, and both approaches were compared. The following conclusions can be obtained from both the mathematical and FE approaches.

1) Skewing the magnets with optimum skew angle is an effective tool to minimize the pulsating torque component in AFPM machines.
2) Replacing the gramme-type rectangular winding with the pie-shaped winding helps reduce the torque ripple component of the slotless topologies by providing better stator utilization.
3) Torque ripple is sensitive to the change of magnet skew angle and pole arc ratio. Using this principle, a torque ripple minimization technique was developed by skewing and choosing the magnet pole arc ratio.
4) Torque ripple sensitivity ratio for PM motors implies that the torque ripple performance of the PM motors will fluctuate due to a small change of the skew angle and pole arc ratio.
5) Precise design and manufacturing of the skew angle and magnet pole arc ratio are very important for high-torque-quality PM motors.
6) Nonslotted PM motors are less sensitive to torque ripple than slotted-type PM motors, which implies that nonslotted topologies are better than the slotted topologies in terms of torque ripple sensitivity.

ACKNOWLEDGMENT

The authors would like to thank Ansoft Corporation for providing the FE software used in this project.

REFERENCES

[1] C. C. Jensen, F. Profumo, and T. A. Lipo, "A low loss permanent magnet brushless DC motor utilizing tape wound amorphous iron," *IEEE Trans. Ind. Appl.*, vol. 28, no. 3, pp. 646–651, May/Jun. 1992.
[2] Z. Zhang, F. Profumo, and A. Tenconi, "Axial flux versus radial flux PM motors," in *Proc. SPEEDAM*, Capri, Italy, 1996, pp. A4-19–A4-25.
[3] S. Huang, M. Aydin, and T. A. Lipo, "Comparison of (non-slotted and slotted) surface mounted PM motors and axial flux motors for submarine ship drives," in *Proc. 3rd Naval Symp. Elect. Mach.*, Dec. 2000.
[4] T. M. Jahns and W. L. Soong, "Pulsating torque minimization techniques for permanent magnet AC motor drives-a review," *IEEE Trans. Ind. Electron.*, vol. 43, no. 2, pp. 321–329, Apr. 1996.
[5] K. Rahman, N. Patel, T. Ward, J. Nagashima, F. Caricchi, and F. Drescimbini, "Application of direct drive wheel motor for fuel cell electric and hybrid electric propulsion," in *Proc. IEEE-IAS 39th Annu. Meeting*, Oct. 2004, pp. 1420–1426.
[6] T. A. Lipo, S. Huang, and M. Aydin, "Performance assessment of axial flux permanent magnet motors for low noise applications," Wisconsin Electrical Machines and Power Electronics Consortium (WEMPEC), Madison, WI, Final Rep. to ONR, Oct. 2000.
[7] S. Huang, M. Aydin, and T. A. Lipo, "Torque quality assessment and sizing optimization for surface mounted PM machines," in *Proc. IEEE-IAS 36th Annu. Meeting*, 2001, pp. 1603–1610.
[8] M. Aydin, S. Huang, and T. A. Lipo, "Optimum design and 3-D finite element analysis of non-slotted and slotted internal rotor type axial flux PM disc machines," in *Proc. IEEE PES Summer Meeting*, Vancouver, BC, Canada, 2001, pp. 1409–1416.
[9] ——, "Design and electromagnetic field analysis of non-slotted and slotted TORUS type axial flux surface mounted disc machines," in *Proc. IEEE Int. Conf. Elect. Mach. Drives*, Boston, MA, 2001, pp. 645–651.

Metin Aydin (S'98–M'04) was born in Turkey. He received the B.S. degree from Istanbul Technical University, Istanbul, Turkey, in 1993, and the M.S. and Ph.D. degrees from the University of Wisconsin, Madison, in 1997 and 2004, respectively, all in electrical engineering.

He was with the Wisconsin Electrical Machines and Power Electronics Consortium for eight years and worked on various projects related to electric motor design. He is currently with Caterpillar Inc., Peoria, IL. His research interests include electrical machine design and control.

Surong Huang was born in Shanghai, China. He received the B.S. and M.S. degrees in electrical engineering from Shanghai University, Shanghai, China.

In 1977, he joined Shanghai University of Technology and was promoted to Associate Professor and Professor in 1993 and 2001, respectively. He was a Visiting Faculty Member in the Department of Electrical and Computer Engineering, University of Wisconsin, Madison, in 1995–1996 and 1998–2000. He has published more than 70 papers concerning the development of new types of electrical machines and drive systems; design, control, modeling, and simulation of electrical machines and alternating current drives; and vibration and noise analysis of electrical machines, which are his research interests.

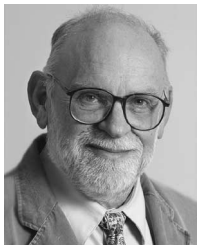

Thomas A. Lipo (M'64–SM'71–F'87) was born in Milwaukee, WI. He received the B.E.E. and M.S.E.E. degrees from Marquette University, Milwaukee, WI, in 1962 and 1964, respectively, and the Ph.D. degree in electrical engineering from the University of Wisconsin, Madison, in 1968.

From 1969 to 1979, he was an Electrical Engineer in the Power Electronics Laboratory, Corporate Research and Development, General Electric Company, Schenectady, NY. He was a Professor of electrical engineering at Purdue University, West Lafayette, IN, in 1979. In 1981, he joined the University of Wisconsin, where he is currently the W. W. Grainger Professor for Power Electronics and Electrical Machines, Co-Director of the Wisconsin Electric Machines and Power Electronics Consortium, Director of the Wisconsin Power Electronics Research Center, and Campus Director of the Center for Power Electronics Systems, which is sponsored by the National Science Foundation. He has published more than 400 technical papers and is the holder of 36 U.S. patents.

Dr. Lipo was the recipient of 26 IEEE prize paper awards from three different IEEE Societies including Best Paper Awards for a publication in the IEEE TRANSACTIONS in the years 1984, 1994, and 1999. He was also the recipient of three major awards from three different IEEE Societies. In 1986, he received the Outstanding Achievement Award from the IEEE Industry Applications Society (IAS) for his "contributions to the field of ac drives." In 1990, he received the William E. Newell Award from the IEEE Power Electronics Society for his "contributions to the field of power electronics." He also received the 1995 Nicola Tesla IEEE Field Award "for pioneering contributions to the simulation of and application to electric machinery in solid-state alternating current motor drives." In 2004, he received the prestigious Hilldale Award from the University of Wisconsin, making him the only member of the Department of Electrical Engineering ever so-honored for his contributions to research. Over a 40-year period, he has served three IEEE Societies in numerous capacities including as President of the IEEE IAS in 1994. He was made a Fellow of the Royal Academy of Engineering (Great Britain) in 2003.